Department of Physics and Astronomy

University of Heidelberg

Master thesis

in Physics

submitted by

Stephan Friedrich Stiefelmaier

born in Kirchheim unter Teck

Improving the Accuracy of the Photon Conversion Method in ALICE

This Master thesis has been carried out by Stephan Friedrich Stiefelmaier

at the

Physikalisches Institut Heidelberg

under the supervision of

apl. Prof. Dr. Klaus Reygers

Abstract

One method to measure neutral mesons and direct photons in ALICE is to reconstruct electron-positron pairs from the conversion of photons in the detector material. This approach currently suffers from a 4 % systematic uncertainty related to the knowledge of the material budget. A reduction of this uncertainty is key for establishing a signal of thermal direct photons at low p_{T} ($1 < p_{\mathrm{T}} < 3$ GeV/c) and for discriminating between models describing direct-photon production in heavy-ion collisions. In this thesis an approach was developed which, has the potential to reduce the material budget uncertainty by calibrating the rest of the detector material using the TPC gas as a well understood reference.

Kurzdarstellung

Eine Methode für die Messung neutraler Pionen und direkter Photonen in ALICE besteht darin, Elektron-Positron Paare zu rekonstruieren, die bei der Konversion von Photonen im Material des Detektors entstehen. Diese Methode hat den momentan den Nachteil, dass mit ihr eine systematische Unsicherheit in der Höhe von 4 % verbunden ist. Diese Unsicherheit ist in der unzureichenden Kenntnis des Materialbudgets von ALICE begründet. Eine Reduzierung dieser Unsicherheit ist unerlässlich wenn man ein Signal thermaler direkter Photonen bei niedrigen p_{T} ($1 < p_{\mathrm{T}} < 3$ GeV/c) messen möchte und zwischen Modellen, welche die Produktion direkter Photonen in Schwerionen Kollisionen beschreiben, unterscheiden möchte. In dieser Arbeit wurde ein Ansatz entwickelt, der das Potential hat die mit dem Materialbudget verbundene Unsicherheit reduzieren zu können. Die Grundidee besteht dabei darin, die TPC als eine gut verstandene Referenz zu verwenden, um den Rest des Materials des Detektors zu kallibrieren.

Contents

Chapter 1

Introduction

One of the questions physicists are trying to answer is the question about the history of the universe. Most of the theories which have been developed in this field of research point to a state of incredibly high energy density shortly after the beginning of the evolution of the universe in which quarks and gluons were present in an atypical unbound state. In scientific language this state of matter is referred to as Quark Gluon Plasma (QGP). The QGP state existed only very shortly since the energy density rapidly decreased due to expansion and radiation processes, allowing the quarks to bind together into hadrons. Stable hadrons – protons and if bound in a nucleus also neutrons – are the building blocks of matter as we experience it in everyday life. On both the experimental and theoretical side, a lot of effort is put into understanding the time evolution of the QGP. The Large Hadron Collider (LHC) at CERN is one of the experimental sites capable of producing QGP states of matter by colliding counter rotating lead nucleus at center of mass energies of up to $\sqrt{s} = 5.5\,\text{TeV}$. If the nucleus collide head-on, the energy density is high enough for the nuclei to disintegrate into a soup of deconfined quarks and gluons, creating a quark-gluon plasma. ALICE (A Large Ion Collider Experiment) is the experiment dedicated for studying properties of the QGP at the LHC. It is designed to be able to reconstruct the tracks of the large amounts of charged particles that are produced in a lead-lead collision. Moreover, it can identify the species of the particles down to low transverse momenta making it a well suited tool for investigating properties of the QGP. Since the lifetime of a QGP is short it can only be studied indirectly, using particles created in the plasma or affected by the plasma on their way out of the collision zone. One way to go is the measurement of thermal photons, photons that are created in the quark-gluon plasma during its thermalization phase. A fraction of the photons converts into electron-positron pairs when traversing the detector. The reconstruction of these photon conversions in order to infer back to the spectra of produced photons is one of the methods used in ALICE for measuring photons and called Photon Conversion Method (PCM). This work is concerned with the systematic uncertainty of the method due to the incomplete knowledge of the material budget within the detector. An aproach is examined to reduce this uncertainty.

Chapter 2

Theoretical Background

2.1 The Standard Model of Particle Physics

The Standard Model of Particle Physics aims at explaining observable phenomena at high energy scales from first principles. To this end, the model defines a set of elementary particles and delivers a mathematical description in which way these elementary particles may interact with each other. In this way, it not only gives the basic ingredients of matter as we experience it in everyday live but also predicts new particles that will only be created under extreme conditions and have a very short lifetime. Behind the term 'elementary' stands the claim that none of these particles has a substructure e.g. is composed of something smaller. Up to today there is no experimental data which contradicts this claim. However, nobody can say with certainty that this claim is in fact true.

The set of elementary particles consists of two fundamentally diffrent kinds of particles: massive spin-$\frac{1}{2}$ fermions on the one hand and integer spin gauge bosons, mediating the forces between the fermions, on the other hand. Figure 2.1 shows the elementary particles along with their classification. The fermion group of particles comprises six quarks (q) and six leptons (l) which are further categorized into three, increasing in mass, generations of matter. Each generation contains two quarks (electrical charges $q = +\frac{2}{3}q_e$, $-\frac{1}{3}q_e$), one negatively charged lepton ($q = -1q_e$) and one electrically neutral lepton-neutrino ν. The quark family members are labeled *up* (u), *down* (d), *charm* (c), *strange* (s), *top* (t), *bottom* (b) with *u, d, s* referred to as light quarks (masses $\approx$ 2.3, 4.8, 95 MeV/c^2) and *c, b, t* as heavy quarks (masses $\approx$ 1.3, 4.2, 173.1 GeV/c^2). The charged leptons are labeled *electron* (e), muon (μ) and tau (τ). Each has an electrically neutral and much lighter neutrino partner (ν_e, ν_μ, ν_τ). For all fermion particles there exists an anti-version with inverted quantum numbers. The first works preparing the ground for the Standard Model were done by Glashow, Weinberg and Salam in the 1960s [1] [2] [3]

2.2 Photons as a probe of the Qark Gluon Plasma

In nature quarks are never observed freely but only in bound states, called hadrons. Since the potential between two quarks grows linearly with distance, once a certain distance is exceeded it becomes energetically more favourable that a quark anti-quark pair is produced from vacuum. At very high temperatures however, hadronic matter undergoes a phase transition into a soup of quasi-free quarks and gluons. This state of matter is called Quark Gluon Plasma (QGP) and is expected to have existed shortly after the Big Bang. It can also be created artificially if nucleus are collided with high center of mass energies, as it

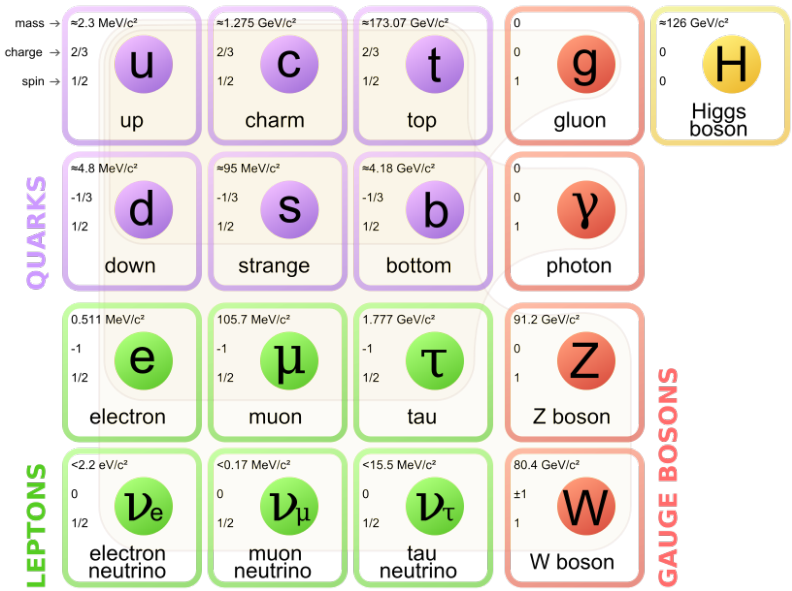

Figure 2.1: The building blocks of matter according to the Standard Model of Particle Physics. Taken from [4]

is done at the LHC with Pb-Pb collisions or at RHIC with Au-Au collisions. Since the lifetime of a QGP is very short it can only be studied indirectly via particles that are created in the QGP or via the distributions of particles that get affected by the QGP. One probe for studying the QGP are photons which have the favorable property that they leave the collision zone mostly unaffected since the electromagnetic coupling constant is small. The photons created in a collision are categorized according to their production mechanism. Photons that are created in a decay of a mother particle are called decay photons and represent the bulk of produced photons. The electromagnetic decay of neutral pions into two photons dominates the spectrum of decay photons. Photons not coming from a decay are called direct photons. It is put a lot of effort into the measurement of the direct photon signal since it carries information about the early stages of the collision. Their spectrum includes high-p_{T} photons produced in hard processes during the initial parton-parton scattering phase whose p_{T}-spectra can be calculated by means of pQCD and in the case of Pb-Pb collisions also includes so called *thermal*-photons, produced in the thermalizing QGP medium by the same strong interaction mechanism but at much lower transferred momentum scales, therefore called soft photons. While the prompt photons are important since they can be tested against pQCD calculations the thermal photons are interesting since they give insight in the mechanisms that rule the QGP.

Chapter 3

Photon Conversion Method

The Photon Conversion Method is one of the methods used for measuring the spectra of produced photons in particle-particle collisions in ALICE at the LHC. The basic principle of the method is to use the fraction of photons which convert into electron-positron pairs in the detector material, which can be tracked by the main ALICE tracking devices in the central barrel. From the bulk of charged particle tracks created in each initial collision the method tries to find those pairs of tracks which originate from a photon conversion and then calculates the properties of the associated photon. Both the conversion and the recombination of electron pairs (short-notation of electron-positron pair) to converted photons are statistical processes depending on p_{T}, making it non-trivial to infer the amount and distribution in p_{T} of the set of produced photons. In this chapter I will give an overview over the method.

3.1 Reconstruction of Converted Photons

3.1.1 V0-finder - general

The reconstruction of converted photons employs a so called V0-finder, an algorithm developed to find secondary vertices such as from strange decays or photon conversions. The algorithm takes as input the set of secondary tracks. These are tracks calculated without the assumption that the track has the primary vertex as a starting point. Figure 3.1 shows a sketch of the method. The algorithm performs the following steps for each pair of oppositely charged tracks: (i) calculate the impact parameters (b, $b+$) with respect to the primary vertex for both tracks. If at least one of (b, $b+$) is below a treshhold discard this pair of tracks and start over with a new one. (ii) Calculate the distance of closest approach (DCA) for the two tracks. Discard the pair if the DCA exceeds a threshold, depending on the distance to the primary vertex and its resolution. The maximum allowed DCA is 1 cm. (iii) Keep the V0 (the obtained secondary vertex) if it lies within the fiducial R-range 0.5–220 cm, indicated by dashed lines in the sketch. (vi) Calculate the angle between the V0 momentum vector (P) (the sum of the track momenta at their DCA) and the vector which points from the primary vertex to the V0 (R). Reject the pair if the cosine of that angle is below 0.85.

There are two V0-finders used, on-fly and offline. The on-fly V0-finder is applied during the reconstruction phase of the data when more information is still available and the tracks can be refitted.

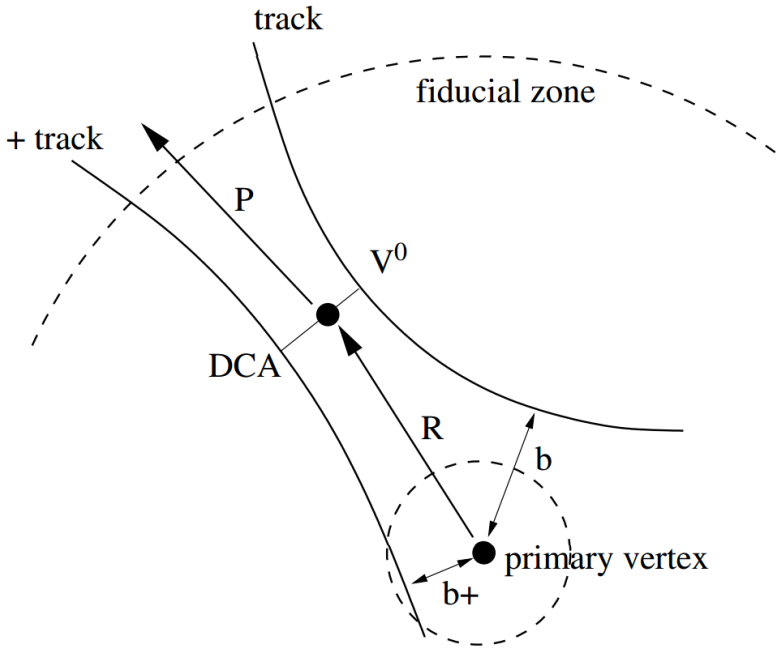

Figure 3.1: Sketch of a V0 reconstruction. Taken from [5]

3.1.2 Photon specific further procedure

The spatial resolution of the reconstructed conversion points can be improved exploiting the fact that in case of a photon conversion the momenta of the electrons need to be almost parallel at their point of creation due to momentum conservation. This procedure is explained in detail in [6]. The obtained set of photon candidates is then filtered for in three steps for various criteria in order to get rid of as many misidentified photon conversion V0s as possible. This is crucial since one would otherwise depend strongly on an identical background in the monte carlo simulations for a correct evaluation of the efficiency. The main sources for misidentified photon conversions are decays of K^0_S, Λ and $\bar{\Lambda}$ on the one hand and random combinations electron and positron tracks on the other hand. In the first step, cuts regarding the reconstruction quality and the spatial orientation of the tracks are applied. In the next step, particle identification cuts are applied, mainly a $\mathrm{d}E/\mathrm{d}X$ cut in the TPC gas. In the last step, cuts are applied which exploit the topology of photon conversions.

3.2 Material Budget Uncertainty

Ultimately, one is interested in the spectrum of produced photons which means that the ratio of reconstructed over produced photons must be determined. This ratio is called photon reconstruction efficiency and is determined from Monte Carlo simulations. The simulations have a three-dimensional map of the detector geometry which ideally contains every piece of hardware of the ALICE detector stored with its position, shape and chemical composition. In the simulations, the material budget map is then used to calculate the

conversion probability of a photon traversing the detector with a given p_{T}. Given the size and complexity of ALICE a map of the material budget can only be accurate up to a certain level. As a consequence, the conversion probability in the simulation will not correspond exactly to the true conversion probability present when data taking and hence will give rise to a deviating photon reconstruction efficiency. Of course, it must be evaluated how good the agreement between the material budget description in MC and the material budget present in the true detector is and what the effects on the final spectra are. The uncertainty on the photon spectra due to this is called material budget uncertainty and at present has a value of about 4.5 %. In the following I outline how the material budget uncertainty currently is determined. A comprehensive description of the method is given in [7]

3.2.1 Current Procedure

In principle, one wants to know whether same produced photon spectra in DATA and MC will lead to same reconstructed photon spectra. Since the numbers of produced photons in DATA is unknown one can not directly compare the ratios of recontructed over produced photon numbers in DATA and MC. Instead, one normalizes the reconstructed photon numbers to the number of charged particle tracks in the same set of events investigated. The assumption here is that the ratio of produced photons over charged particles is described by simulations so well, that diffrences seen between DATA and MC will reflect diffrences in the photon conversion probabilities. One then calculates the quantity d_γ:

$$d_\gamma = \left(\frac{N_\gamma^{\mathrm{reco}}}{N_{\mathrm{ch}}}\right)^{\mathrm{DATA}} - \left(\frac{N_\gamma^{\mathrm{reco}}}{N_{\mathrm{ch}}}\right)^{\mathrm{MC}} \tag{3.1}$$

In this equation N_γ^{reco} stands for the sum of all reconstructed photons which have a conversion radius smaller than 180cm. d_γ is interpreted as a measure which reflects how well conversion probability for photons in the simulation agrees with the real world. The quantity is of course also sensitive to diffrences between DATA and MC in the V0 finding efficiency. To estimate this effect on d_γ the V0 finder is varied between offline and on-fly. To get an estimate, how robust the initial assumption of equal ratios of produced photons over charged particles in DATA and MC is, the event generators in the simulation are varied between Pythia and Phojet and also the p_{T}-range when calculating N_γ^{reco} is varied between all p_{T} and a fiducial range 1.0 - 3.0 GeV/c. For d_γ the average of PHOJET and PYTHIA is taken and the variations are then combined to an overall uncertainty on d_γ. The sum of d_γ and its uncertainty is then taken as the total material budget uncertainty.

Generator LHC10[b,c]	V0-finder	full p_T Error [%]	mid p_T Error [%]
Phojet	Onfly	2.57	5.58
	Offline	1.56	2.06
Pythia	Onfly	-0.90	-8.48
	Offline	-2.19	-11.07

Generator LHC10[d,e,h]	V0-finder	full p_T Error [%]	mid p_T Error [%]
Phojet	Onfly	3.69	9.14
	Offline	3.49	7.69
Pythia	Onfly	0.33	-5.37
	Offline	-0.05	-6.31

Table 3.1: Error calculation for different particle generators (Phojet / Pythia), two V0-finders (Onfly/ Offline) and p_T-ranges for the photon (full p_T and intermediate p_T ($1.0 - 3.0$ GeV/c). The differences are always Data - MC in % of MC. Taken from [7]

value	LHC10[b,c]	LHC10[d,e,h]
d_γ^{abs}	0.83%	2.01%
$\Delta d_\gamma^{\text{Gen}}$	2.45%	2.37%
$\Delta d_\gamma^{\text{V0-finder}}$	0.71%	0.14%
$\Delta d_\gamma^{p_T}$	0.87%	1.57%
Δ_{Mat}	3.53%	4.86%

Table 3.2: Final systematic error estimate of the material budget for the different samples.Taken from [7]

The following equations illustrate the procedure:

$$d_\gamma^{\text{abs}} = \frac{d_\gamma^{\text{Phojet, On-the-Fly all } p_T} + d_\gamma^{\text{Pythia, On-the-Fly, all } p_T}}{2} \tag{3.2}$$

$$\Delta d_\gamma^{\text{Gen}} = |d_\gamma^{\text{Phojet, On-the-Fly, all } p_T} - d_\gamma^{\text{Pythia, On-the-Fly, all } p_T}|/\sqrt{2} \tag{3.3}$$

$$\Delta d_\gamma^{\text{V0-finder}} = \left| d_\gamma^{\text{Phojet, On-the-Fly, all } p_T} - d_\gamma^{\text{Phojet, Offline, all } p_T} \right| /\sqrt{2} \tag{3.4}$$

$$\Delta d_\gamma^{p_T} = \left| d_\gamma^{\text{Phojet, On-the-Fly, all } p_T} - d_\gamma^{\text{Phojet, On-the-Fly, mid } p_T} \right| /\sqrt{12} \tag{3.5}$$

$$\Delta d_\gamma^{\text{abs}} = \sqrt{\left(\Delta d_\gamma^{\text{Gen}}\right)^2 + \left(\Delta d_\gamma^{\text{V0-finder}}\right)^2 + \left(\Delta d_\gamma^{p_T}\right)^2} \tag{3.6}$$

$$\Delta_{\text{Mat}} = d_\gamma^{\text{abs}} + \Delta d_\gamma^{\text{abs}} \tag{3.7}$$

Table 3.1 and table 3.2 give an overview over the contributions to the material budget uncertainty in its current form.

3.2.2 Key Aspects of Current Procedure

From table 3.2 we see that about half of the total material budget uncertainty comes from the contribution $\Delta d_{\gamma}^{\mathrm{Gen}}$. At first order, (for pp-collisions [1]) this contribution reflects how the ratio of produced photons over charged particles differs in PYTHIA and PHOJET. It is believed that the agreement between both generators in this variable is at the same order as the agreement of the mean of both with DATA. As a consequence $\Delta d_{\gamma}^{\mathrm{Gen}}$ establishes a level of confidence for the normalization with charged particles. To summarize, half of the material budget uncertainty comes from the normalization to charged particles. When extracting the photon reconstruction efficiency from the MC simulations it is however only of secondary importance to have the exact same ratio of photons over charged particles as in DATA. Since we divide by the total number of produced photons in the calculation of the efficiency, diffrent input photon spectra compared to DATA do only a have a subordinated effect on the efficiency. If there is another way for comparing the number of conversion in DATA and MC that does not use the normalization to charged particles the material budget uncertainty can be reduced. One possibility could be the use of a certain region of the detector where the knowledge of the material budget is particularly good. Such a region could serve for callibrating the rest of the material budget and by that reduce the uncertainty. The investigation and testing of this idea is the main topic of this thesis.

[1] for pp-collisions the multiplicity is low compared to what ALICE is designed for and hence the efficiency is flat to good approximation [**analysisNote**]

Chapter 4

Investigating the Weights Idea

It was pointed out in the previous chapter, that discrepancies between the physical detector description in MC with respect to the true detector lead to biases on the photon reconstruction efficiencies. In this chapter an idea is developed, how such discrepancies can be identified and corrected for when workin with existing MC productions. On long terms, new MC productions should then be based on a corrected material budget description. As a guiding principle to find out how such corrections could be done when working with existing MC productions, we can ask, what needs to be done that the output of an analysis task run on a MC production is such as if the true material budget had been used.

4.1 A simple model of the PCM

We have seen in the previous subchapter that it is crucial that the photon reconstruction efficiency as it is determined in MC is equal to the efficiency in DATA. The reconstruction efficiency in MC is determined as

$$\epsilon_{\gamma}^{\mathrm{reco,MC}}\left(p_{\mathrm{T}}\right) = \frac{N_{\gamma}^{\mathrm{reco,MC}}\left(p_{\mathrm{T}}\right)}{N_{\gamma}^{\mathrm{prod,MC}}\left(p_{\mathrm{T}}\right)} \tag{4.1}$$

Note that nearly throughout the whole thesis (p_{T}) is to be understood as a bin with finite widht. Strictly speaking, $\epsilon_{\gamma}^{\mathrm{reco,MC}}\left(p_{\mathrm{T}}\right)$ is determined as the outcome of a random experiment in which the ratio of two correlated binomial distributions is calculated. What we ideally would like to have, is that the expectation values of $\epsilon_{\gamma}^{\mathrm{reco,MC}}\left(p_{\mathrm{T}}\right)$ and $\epsilon_{\gamma}^{\mathrm{reco}}\left(p_{\mathrm{T}}\right)$ coincide. We now want to see how deviations in the mc material budget description lead to a mismatch of these expectation values. To this end, we approximate

$$\left\langle \epsilon_{\gamma}^{\mathrm{reco,MC}}\left(p_{\mathrm{T}}\right)\right\rangle = \left\langle \frac{N_{\gamma}^{\mathrm{reco,MC}}\left(p_{\mathrm{T}}\right)}{N_{\gamma}^{\mathrm{prod,MC}}\left(p_{\mathrm{T}}\right)}\right\rangle = \frac{\left\langle N_{\gamma}^{\mathrm{reco,MC}}\left(p_{\mathrm{T}}\right)\right\rangle}{N_{\gamma}^{\mathrm{prod,MC}}\left(p_{\mathrm{T}}\right)} \tag{4.2}$$

$$= \sum_{r_i} p_{\mathrm{r}}^{\mathrm{MC}}\left(r_i, p_{\mathrm{T}}\right) \cdot p_{\mathrm{c}}^{\mathrm{MC}}\left(r_i, p_{\mathrm{T}}\right) \cdot \epsilon_{\mathrm{V0}}^{\mathrm{MC}}\left(r_i, p_{\mathrm{T}}\right) \tag{4.3}$$

In this equation $p_{\mathrm{r}}\left(r_i, p_{\mathrm{T}}\right)$ stands for the probability that a photon with given p_{T} reaches radial bin r_i, $p_{\mathrm{c}}\left(r_i, p_{\mathrm{T}}\right)$ denotes the probability that it converts in r_i and $\epsilon_{\mathrm{V0}}\left(r_i, p_{\mathrm{T}}\right)$ stands for the probability that a photon which has converted in r_i gets reconstructed by the V0 finder.

We now express all MC quantities in terms of the true quantities and a factor describing the actual deviation:

$$\left\langle \epsilon_\gamma^{\mathrm{reco,MC}}\left(p_\mathrm{T}\right)\right\rangle = \sum_{r_i} f_\mathrm{off}^{p_\mathrm{r}}\left(r_i,p_\mathrm{T}\right)\, p_\mathrm{r}\left(r_i,p_\mathrm{T}\right)\cdot f_\mathrm{off}^{p_\mathrm{c}}\left(r_i,p_\mathrm{T}\right)\, p_\mathrm{c}\left(r_i,p_\mathrm{T}\right)\cdot f_\mathrm{off}^{\epsilon_\mathrm{V0}}\left(r_i,p_\mathrm{T}\right)\, \epsilon_\mathrm{V0}\left(r_i,p_\mathrm{T}\right) \tag{4.4}$$

where $f_\mathrm{off}^{p_\mathrm{r}}\left(r_i,p_\mathrm{T}\right)$ is completely determined by $p_\mathrm{c}\left(r_i,p_\mathrm{T}\right)$ and $f_\mathrm{off}^{p_\mathrm{c}}\left(r_i,p_\mathrm{T}\right)$. We now want to see if radially dependent correction factors $f_\mathrm{corr}\left(r_i\right)$ could be used to correct for the deviations when determining $\epsilon_\gamma^{\mathrm{reco,MC}}\left(p_\mathrm{T}\right)$:

$$\epsilon_\gamma^{\mathrm{reco,MC}}\left(p_\mathrm{T}\right) = \frac{\sum\limits_{r_i} f_\mathrm{corr}\left(r_i\right)\cdot N_\gamma^{\mathrm{reco,MC}}\left(r_i,p_\mathrm{T}\right)}{N_\gamma^{\mathrm{prod,MC}}\left(p_\mathrm{T}\right)} \tag{4.5}$$

Then

$$\left\langle \epsilon_\gamma^{\mathrm{reco,MC}}\left(p_\mathrm{T}\right)\right\rangle = \sum_{r_i} f_\mathrm{corr}\left(r_i\right)\cdot\left(f_\mathrm{off}^{p_\mathrm{r}} f_\mathrm{off}^{p_\mathrm{c}} f_\mathrm{off}^{\epsilon_\mathrm{V0}}\right)\left(r_i,p_\mathrm{T}\right)\cdot\left(p_\mathrm{r}\, p_\mathrm{c}\, \epsilon_\mathrm{V0}\right)\left(r_i,p_\mathrm{T}\right) \tag{4.6}$$

Ideally, the set of only r-dependent correction factors $f_\mathrm{corr}\left(r_i\right)$ is chosen such, that it corrects for the product of all present MC deviations $\left(f_\mathrm{off}^{p_\mathrm{r}} f_\mathrm{off}^{p_\mathrm{c}} f_\mathrm{off}^{\epsilon_\mathrm{V0}}\right)\left(r_i,p_\mathrm{T}\right)$. With such an ideal set of correction factors one can write

$$\left\langle \epsilon_\gamma^{\mathrm{reco,MC}}\left(p_\mathrm{T}\right)\right\rangle = \sum_{r_i} f_\mathrm{corr}^{\mathrm{ideally}}\left(r_i\right)\cdot\left(f_\mathrm{off}^{p_\mathrm{r}} f_\mathrm{off}^{p_\mathrm{c}} f_\mathrm{off}^{\epsilon_\mathrm{V0}}\right)\left(r_i,p_\mathrm{T}\right)\cdot\left(p_\mathrm{r}\, p_\mathrm{c}\, \epsilon_\mathrm{V0}\right)\left(r_i,p_\mathrm{T}\right) \tag{4.7}$$

$$= \sum_{r_i}\left(p_\mathrm{r}\, p_\mathrm{c}\, \epsilon_\mathrm{V0}\right)\left(r_i,p_\mathrm{T}\right) \tag{4.8}$$

$$= \epsilon_\gamma^{\mathrm{reco}}\left(p_\mathrm{T}\right) \tag{4.9}$$

Equation 4.8 can be seen as a set of equations which define the set of ideal correction factors $f_\mathrm{corr}^{\mathrm{ideally}}\left(r_i\right)$. As this set of equations is substantially important for this work lets write it down explecitly:

$$\sum_{r_i} f_\mathrm{corr}^{\mathrm{ideally}}\left(r_i\right)\cdot\left(f_\mathrm{off}^{p_\mathrm{r}} f_\mathrm{off}^{p_\mathrm{c}} f_\mathrm{off}^{\epsilon_\mathrm{V0}}\right)\left(r_i,p_\mathrm{T}\right)\cdot\left(p_\mathrm{r}\, p_\mathrm{c}\, \epsilon_\mathrm{V0}\right)\left(r_i,p_\mathrm{T}\right) = \sum_{r_i}\left(p_\mathrm{r}\, p_\mathrm{c}\, \epsilon_\mathrm{V0}\right)\left(r_i,p_\mathrm{T}\right) \tag{4.10}$$

That equation 4.10 can hold for every p_T bin the number of radial bin r_i must be greater or equal to the number of p_T-bins. We know now, that if $\left(f_\mathrm{off}^{p_\mathrm{r}} f_\mathrm{off}^{p_\mathrm{c}} f_\mathrm{off}^{\epsilon_\mathrm{V0}}\right)\left(r_i,p_\mathrm{T}\right)$ was known one could in principle solve equation 4.10 for $f_\mathrm{corr}^{\mathrm{ideally}}\left(r_i\right)$ and by applying those in the analysis chain correct for an inaccurate material budget description.

The question remains what is the best way to obtain a set of correction factors $f_\mathrm{corr}\left(r_i\right)$ which is as close as possible to the ideal set $f_\mathrm{corr}^{\mathrm{ideally}}\left(r_i\right)$. In the next subsection I discuss the idea of using 'normal' weights as correction factors.

4.2 Using Normal Weights

The basic idea of the weights approach was to use radially defined correction factors w_i defined as

$$w_i = \frac{\left(\sum_{p_\mathrm{T}} N_\gamma^{\mathrm{reco}}(r_i, p_\mathrm{T}) \Big/ \sum_{p_\mathrm{T}} N_\gamma^{\mathrm{reco}}(r_x, p_\mathrm{T}) \right)^{\mathrm{DATA}}}{\left(\sum_{p_\mathrm{T}} N_\gamma^{\mathrm{reco}}(r_i) \Big/ \sum_{p_\mathrm{T}} N_\gamma^{\mathrm{reco}}(r_x, p_\mathrm{T}) \right)^{\mathrm{MC}}} \tag{4.11}$$

where r_x is an radial bin that we use for callibrating the rest of the detector volume, e.g. we think that the MC material budget description in r_x is particularly good.
Write down the expectation values for w_i:

$$\langle w_i \rangle = \frac{\sum_{p_\mathrm{T}} N_\gamma^{\mathrm{prod}}(p_\mathrm{T}) \cdot (p_\mathrm{r}\, p_\mathrm{c}\, \epsilon_{\mathrm{V0}})(r_i, p_\mathrm{T})}{\sum_{p_\mathrm{T}} N_\gamma^{\mathrm{prod,MC}}(p_\mathrm{T}) \cdot \left(p_\mathrm{r}^{\mathrm{MC}}\, p_\mathrm{c}^{\mathrm{MC}}\, \epsilon_{\mathrm{V0}}^{\mathrm{MC}}\right)(r_i, p_\mathrm{T})} \cdot \frac{\sum_{p_\mathrm{T}} N_\gamma^{\mathrm{prod,MC}}(p_\mathrm{T}) \cdot \left(p_\mathrm{r}^{\mathrm{MC}}\, p_\mathrm{c}^{\mathrm{MC}}\, \epsilon_{\mathrm{V0}}^{\mathrm{MC}}\right)(r_x, p_\mathrm{T})}{\sum_{p_\mathrm{T}} N_\gamma^{\mathrm{prod}}(p_\mathrm{T}) \cdot (p_\mathrm{r}\, p_\mathrm{c}\, \epsilon_{\mathrm{V0}})(r_x, p_\mathrm{T})} \tag{4.12}$$

4.2.1 Fully Ideal Approximations

I now want to show a set of approximations under which the w_i as defined in equation 4.11 perfectly fullfill the requirements for a set of correction factors in equation 4.10.

1. the shapes of N_γ^{prod} and $N_\gamma^{\mathrm{prod,MC}}$ are identical: $N_\gamma^{\mathrm{prod,MC}}(p_\mathrm{T}) = f_{\mathrm{off}}^{N_\gamma^{\mathrm{prod}}} \cdot N_\gamma^{\mathrm{prod}}(p_\mathrm{T})$
2. neglect effects on 'reaching'-probabilities: $p_\mathrm{r}^{\mathrm{MC}} = p_\mathrm{r} \rightarrow f_{\mathrm{off}}^{p_\mathrm{r}} = 1$
3. the MC deviation of p_c only depends on $r \rightarrow f_{\mathrm{off}}^{p_\mathrm{c}}(r_i, p_\mathrm{T}) = f_{\mathrm{off}}^{p_\mathrm{c}}(r_i)$
4. in r_x the MC material budget description is correct: $p_\mathrm{c}^{\mathrm{MC}}(r_x, p_\mathrm{T}) = p_\mathrm{c}(r_x, p_\mathrm{T})$
5. allow for an r-dependent MC deviation of ϵ_{V0} for $i \neq x$:
   $f_{\mathrm{off}}^{\epsilon_{\mathrm{V0}}}(r_i, p_\mathrm{T}) = f_{\mathrm{off}}^{\epsilon_{\mathrm{V0}}}(r_i)$ with $f_{\mathrm{off}}^{\epsilon_{\mathrm{V0}}}(r_x) = 1$

If we take these approximations we can reformulate equation 4.12 into

$$\langle w_i \rangle = \frac{1}{f_{\mathrm{off}}^{N_\gamma^{\mathrm{prod}}} \cdot f_{\mathrm{off}}^{\epsilon_{\mathrm{V0}}}(r_i) \cdot f_{\mathrm{off}}^{p_\mathrm{c}}(r_i)} \cdot \frac{\sum_{p_\mathrm{T}} N_\gamma^{\mathrm{prod}}(p_\mathrm{T}) \cdot (p_\mathrm{r}\, p_\mathrm{c}\, \epsilon_{\mathrm{V0}})(r_i, p_\mathrm{T})}{\sum_{p_\mathrm{T}} N_\gamma^{\mathrm{prod}}(p_\mathrm{T}) \cdot (p_\mathrm{r}\, p_\mathrm{c}\, \epsilon_{\mathrm{V0}})(r_i, p_\mathrm{T})} \tag{4.13}$$

$$\cdot \frac{f_{\mathrm{off}}^{N_\gamma^{\mathrm{prod}}} \cdot \sum_{p_\mathrm{T}} N_\gamma^{\mathrm{prod}}(p_\mathrm{T}) \cdot (p_\mathrm{r}\, p_\mathrm{c}\, \epsilon_{\mathrm{V0}})(r_x, p_\mathrm{T})}{\sum_{p_\mathrm{T}} N_\gamma^{\mathrm{prod}}(p_\mathrm{T}) \cdot (p_\mathrm{r}\, p_\mathrm{c}\, \epsilon_{\mathrm{V0}})(r_x, p_\mathrm{T})} \tag{4.14}$$

$$= \frac{1}{f_{\mathrm{off}}^{p_\mathrm{c}}(r_i) \cdot f_{\mathrm{off}}^{\epsilon_{\mathrm{V0}}}(r_i)} \tag{4.15}$$

It is obvious that under the approximations we made the $\langle w_i \rangle$ provide a set of ideal correction factors $f_{\text{corr}}^{\text{ideally}}(r_i)$ in equation 4.10.

4.2.2 More Realistic Approximations – $f_{\text{off}}^{\epsilon_{\text{V0}}}(r_x) \neq 1$

To go one step further, we investigate the scenario in which also for r_x the MC V0-efficiency deviates from the data efficiency. Let us hence take the following set of approximations:

1. to 4. same as above
5. $f_{\text{off}}^{\epsilon_{\text{V0}}}(r_i, p_{\text{T}}) = f_{\text{off}}^{\epsilon_{\text{V0}}}(r_i)$, $f_{\text{off}}^{\epsilon_{\text{V0}}}(r_x) \neq 1$

The expectation value for weight w_i will yield

$$\langle w_i \rangle = \frac{1}{f_{\text{off}}^{p_{\text{c}}}(r_i)} \cdot \frac{f_{\text{off}}^{\epsilon_{\text{V0}}}(r_x)}{f_{\text{off}}^{\epsilon_{\text{V0}}}(r_i)} \tag{4.16}$$

And the observed MC photon reconstruction efficiency will be:

$$\left\langle \epsilon_\gamma^{\text{reco,MC}}(p_{\text{T}}) \right\rangle^{\text{ww}} = \sum_{r_i} w_i \cdot \left(f_{\text{off}}^{p_{\text{c}}} f_{\text{off}}^{\epsilon_{\text{V0}}} \right)(r_i) \cdot \epsilon_\gamma^{\text{reco}}(r_i, p_{\text{T}}) \tag{4.17}$$

$$= \sum_{r_i} f_{\text{off}}^{\epsilon_{\text{V0}}}(r_x) \cdot \epsilon_\gamma^{\text{reco}}(r_i, p_{\text{T}}) \tag{4.18}$$

$$= \epsilon_\gamma^{\text{reco}}(p_{\text{T}}) \cdot f_{\text{off}}^{\epsilon_{\text{V0}}}(r_x) \tag{4.19}$$

Where we abbreviated $\epsilon_\gamma^{\text{reco}}(r_i, p_{\text{T}}) = (p_{\text{r}}\, p_{\text{c}}\, \epsilon_{\text{V0}})(r_i, p_{\text{T}})$. The photon reconstruction efficiency as determined from MC will hence be off by a factor $f_{\text{off}}^{\epsilon_{\text{V0}}}(r_x)$.

In order to make a statement whether using the weights improves the accuracy of the final, measured spectra it makes sense to look on the expectation value for $\epsilon_\gamma^{\text{reco,MC}}(p_{\text{T}})$ that one would get without the weights:

$$\left\langle \epsilon_\gamma^{\text{reco,MC}}(p_{\text{T}}) \right\rangle^{\text{nw}} = \sum_{r_i} \left(f_{\text{off}}^{p_{\text{c}}} f_{\text{off}}^{\epsilon_{\text{V0}}} \right)(r_i) \cdot \epsilon_\gamma^{\text{reco}}(r_i, p_{\text{T}}) \tag{4.20}$$

$$= \epsilon_\gamma^{\text{reco}}(p_{\text{T}}) \cdot \sum_{r_i} \left(f_{\text{off}}^{p_{\text{c}}} f_{\text{off}}^{\epsilon_{\text{V0}}} \right)(r_i) \cdot P_{\epsilon_\gamma^{\text{reco}}}(r_i, p_{\text{T}}) \tag{4.21}$$

with $P_{\epsilon_\gamma^{\text{reco}}}(r_i, p_{\text{T}})$ being the proportion to the total photon reconstruction efficiency $\epsilon_\gamma^{\text{reco}}(p_{\text{T}})$ from radial bin r_i:

$$P_{\epsilon_\gamma^{\text{reco}}}(r_i, p_{\text{T}}) = \frac{\epsilon_\gamma^{\text{reco}}(r_i, p_{\text{T}})}{\sum_{r_i} \epsilon_\gamma^{\text{reco}}(r_i, p_{\text{T}})} = \frac{\epsilon_\gamma^{\text{reco}}(r_i, p_{\text{T}})}{\epsilon_\gamma^{\text{reco}}(p_{\text{T}})} \tag{4.22}$$

From these equations we can conclude that:

1. If $f_{\text{off}}^{\epsilon_{\text{V0}}}(r_x)$ is much closer to unity then the weighted sum of $\left(f_{\text{off}}^{p_{\text{c}}} f_{\text{off}}^{\epsilon_{\text{V0}}} \right)(r_i)$ in equation 4.21 the weights have a positive effect on the outcome of the measurement

2. One can only take assumptions about the actual deviations and then evaluate numerically how weights approach compares with not using the weights

3. That way, one can also investigate how deviations from the maybe too idealistic approximations we took (identical p_{T}-shape on input photon spectrum in data and MC, neglectable diffrences in p_{r} between data and MC) propagate in the whole analysis chain

4.3 Evaluation of the Systematic Uncertainties

In this section it is investigated how robustly the weights approach works if one replaces the approximations taken in the last section by real-world scenarios in which the approximations are valid up to a certain point only. To this end, a model was created in which both the DATA and MC quantities are known. The model allows then to simulate the measurement of the photon reconstruction efficiency from MC and to compare the measured MC efficiency to the DATA efficiency and hence to determine the systematic error which would have been done. To obtain the DATA quantities, the conversion probability $p_{\mathrm{c}}\left(r_i, p_{\mathrm{T}}\right)$ and the photon reconstruction efficiency $\epsilon_{\gamma}^{\mathrm{reco}}\left(r_i, p_{\mathrm{T}}\right)$ were extracted from an existing MC production. From $p_{\mathrm{c}}\left(r_i, p_{\mathrm{T}}\right)$ the reaching probabilities $p_{\mathrm{r}}\left(r_i, p_{\mathrm{T}}\right)$ for a given radial bin were calculated by multiplying the counter probabilities $1.0 - p_{\mathrm{c}}\left(r_i, p_{\mathrm{T}}\right)$ for all bins inwards of the given bin. The spectrum of produced photons $N_{\gamma}^{\mathrm{prod}}\left(p_{\mathrm{T}}\right)$ was obtained by extracting the spectrum of produced π^0 mesons, $N_{\pi^0}^{\mathrm{prod}}\left(p_{\mathrm{T}}\right)$ and then using numerical integration of $g\left(p_{\mathrm{T}},\, p_{\mathrm{T},\,\pi^0}\right) \cdot N_{\pi^0}^{\mathrm{prod}}(p_{\mathrm{T},\,\pi^0})$, with $g\left(p_{\mathrm{T}},\, p_{\mathrm{T},\,\pi^0}\right)$ defined as:

$$g\left(p_{\mathrm{T}},\, p_{\mathrm{T},\,\pi^0}\right) = \begin{cases} \frac{2}{p_{\mathrm{T},\,\pi^0}} & , \quad p_{\mathrm{T}} < p_{\mathrm{T},\,\pi^0} \\ 0 & , \quad \text{else} \end{cases} \tag{4.23}$$

which specifies to good approximation[1] the probability density for observing a photon with transverse momentum p_{T} after a π^0 decay which had transverse momentum $p_{\mathrm{T},\,\pi^0}$.

In a next step, MC quantities were created from the DATA quantities introducing deviations. The MC conversion probabilities $p_{\mathrm{c}}^{\mathrm{MC}}\left(r_i, p_{\mathrm{T}}\right)$ were obtained using the inverse of the weights w_i, tag 160 in figure 5.4

In a last step, one can calculate expectation values of reconstructed photon numbers $\left\langle N_{\gamma}^{\mathrm{reco}}\left(r_i, p_{\mathrm{T}}\right)\right\rangle$ by multiplying the spectrum of produced photons with the grid of photon reconstruction efficiencies $\epsilon_{\gamma}^{\mathrm{reco}}\left(r_i, p_{\mathrm{T}}\right)$ both in DATA and MC, calculate the weights according to equation 4.11, and finally compute the expectation value for the observed photon reconstruction efficiencies with and without using the weights, according to equation 4.4

4.3.1 Effect of reaching probabilities p_{r}

To evaluate the systematic error of the weights approach arising from the fact that also the reaching probabilities will be affected by a deviating material budget in MC the model

[1] This holds due to the isotropical distribution of the line on which the photons fly away from the π^0 in the π^0's rest frame.

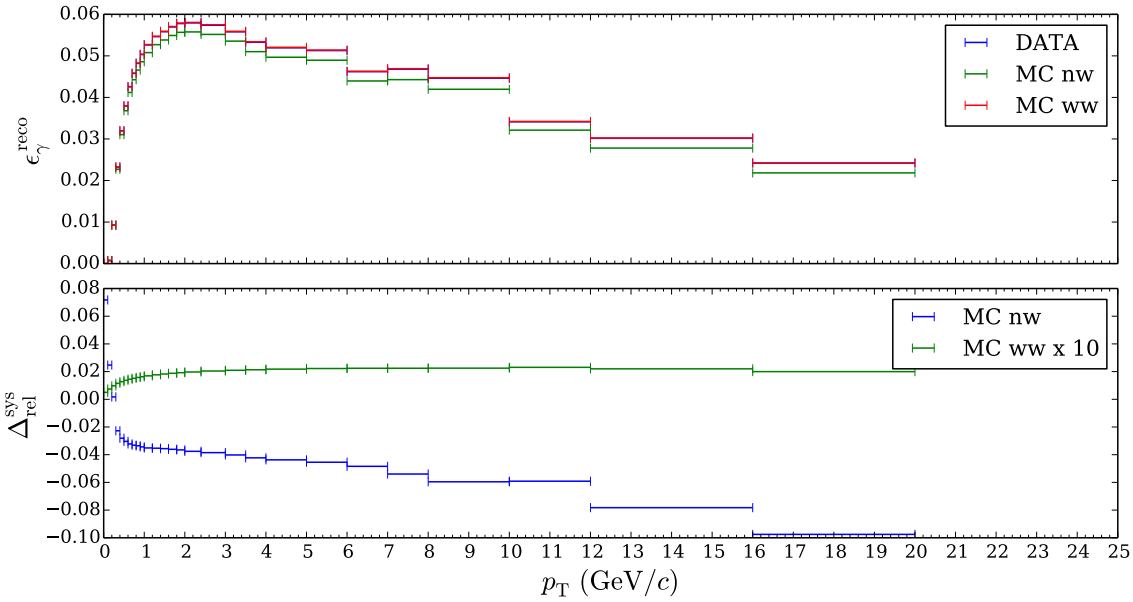

Figure 4.1: Top panel: Photon reconstruction efficiencies in DATA, MC without weights and MC with weights. In a model of the PCM in which the deviations of the MC material budget are given by the inverse of the weights w_i, tag 160 in figure 5.4. Identical photon input spectra in DATA and MC. Bottom panel: relative deviations of the observed MC efficiencies from the DATA efficiency. MC ww has been scaled by a factor of ten before drawn.

was tuned such that the input π^0 spectra (and with that the photon spectra) were equal in DATA and MC.

The top panel of figure 4.1 shows the photon reconstruction efficiencies as one would observe them in MC with (ww) and without (nw) using the weights, along with efficiency in DATA which one would like to observe. The bottom panel displays the deviations of the MC observed efficiencies from the DATA efficiency in units of the DATA efficiency. As such, the (nw) markers display the relative systematic error on the photon reconstruction efficiency caused by an inaccurate material budget description in MC. It is remarkable that the effect has a strong p_{T} dependence at low p_{T} and even flips the sign. This can be explained by the fact, that the p_{T}-shape of the V0 reconstuction efficiency changes with R, see section 6.1.3 for a detailed explanation. The (ww) markers display the relative systematic error on the photon reconstruction efficiency when using the weights. Since it is in the order of 2 per mille it was scaled by a factor of 10 before drawing. It is non-zero due to the effect of the reaching probabilities p_{r}. With r_x being next to the outermost radial bin (see next chapter), a too low material budget in one of the inner bins enters twice when determining the weights. Firstly, in $N_\gamma^{\mathrm{reco,MC}}(r_i, p_{\mathrm{T}})$ by the same factor $f_{\mathrm{off}}^{p_{\mathrm{c}}}(r_i)$ by which the conversion probability in MC with respect to DATA deviates. Secondly, in $N_\gamma^{\mathrm{reco,MC}}(r_x, p_{\mathrm{T}})$ because less conversions at low R lead to more photons reaching higher R. The second effect is subordinated since the probabilities for not converting $1 - f_{\mathrm{off}}^{p_{\mathrm{c}}}(r_i)\, p_{\mathrm{c}}(r_i, p_{\mathrm{T}})$ are not

proportional to $f_{\text{off}}^{p_{\text{c}}}(r_i)$ anymore. As a result, the weights get slightly larger than the inverse of $f_{\text{off}}^{p_{\text{c}}}(r_i)$ (for $f_{\text{off}}^{p_{\text{c}}}(r_i) < 1$).

Consider now $f_{\text{off}}^{p_{\text{r}}}(r_i, p_{\text{T}})$ which describes how the reaching probability in MC deviates from the one in DATA.

$$f_{\text{off}}^{p_{\text{r}}}(r_i, p_{\text{T}}) = \frac{p_{\text{r}}^{\text{MC}}(r_i, p_{\text{T}})}{p_{\text{r}}(r_i, p_{\text{T}})} = \frac{\Pi_{j=0}^{i-1}(1 - f_{\text{off}}^{p_{\text{c}}}(r_j)\ p_{\text{c}}(r_j, p_{\text{T}}))}{\Pi_{j=0}^{i-1}(1 - p_{\text{c}}(r_j, p_{\text{T}}))} \tag{4.24}$$

Thus, $f_{\text{off}}^{p_{\text{r}}}(r_i, p_{\text{T}})$ gets larger than one for $f_{\text{off}}^{p_{\text{c}}}(r_i)$ smaller than one and depends on p_{T}. The larger p_{T} the more $f_{\text{off}}^{p_{\text{r}}}(r_i, p_{\text{T}})$ deviates from unity for a given set of $f_{\text{off}}^{p_{\text{c}}}(r_i)$. To fully correct the number of conversions in a given radial bin one would have to correct by

$$f_{\text{corr}} = \frac{1}{f_{\text{off}}^{p_{\text{r}}}(r_i, p_{\text{T}}) \cdot f_{\text{off}}^{p_{\text{c}}}(r_i, p_{\text{T}})} \tag{4.25}$$

The applied corrections in terms of the weights w_i are thus too large. This effects increases with p_{T}.

4.3.2 Effect of deviating gamma input spectra

To estimate the systematic uncertainty arising from the fact that the input photon spectra might have a diffrent shape, the produced π^0 spectrum in MC was varied. Below 0.7 GeV/c the spectrum was scaled constantly 25% down and above 0.7 GeV/c the spectrum was scaled 25% constantly up. The point of the jump was chosen such that the effect on the systematic error was maximized. Figure 4.2 shows the effect of the introduced discrepancy between the input photon spectra.

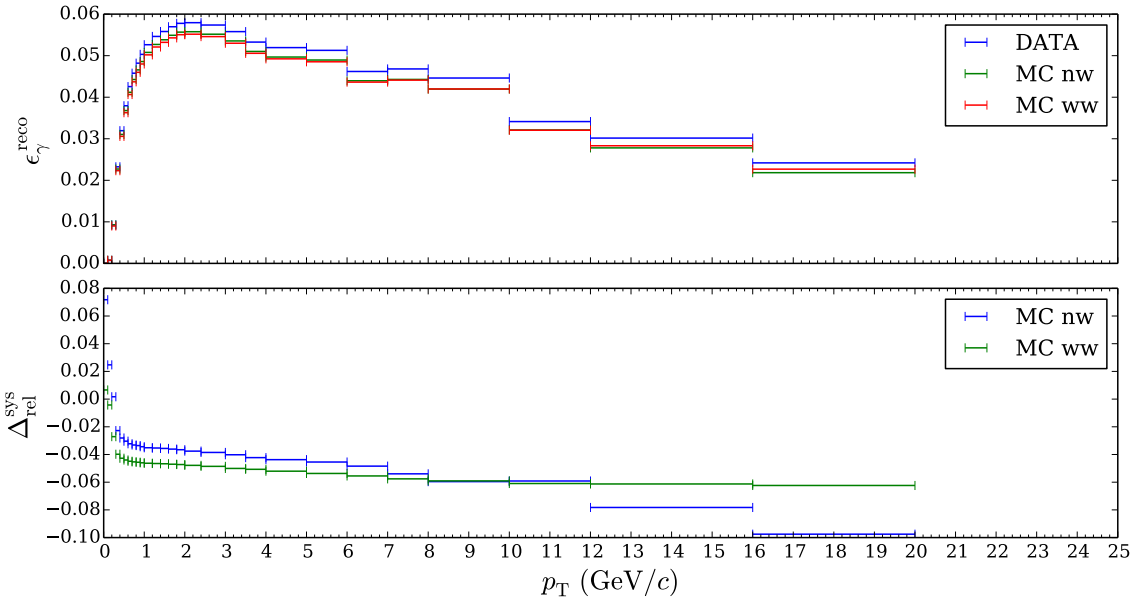

Figure 4.2: Top panel: Photon reconstruction efficiencies in DATA, MC without weights and MC with weights. In a model of the PCM in which the deviations of the MC material budget are given by the inverse of the weights w_i, tag 160 in figure 5.4. The photon spectra differ. Bottom panel: relative deviations of the observed MC efficiencies from the DATA efficiency.

Chapter 5

Determination of the weights

In this chapter I present how the weights were determined. Let me briefly recapitulate the idea of the weights approach. The main idea of the weights approach is to define radial bins r_i and to quantify for each radial bin the discrepancy of the photon conversion probabilities between the true detector and the monte carlo simulation in terms of weights w_i. This is achieved by making use of the fact, that there is a radial bin (denoted by x in equation 5.1) for which the material budget description in MC (and with that the conversion probability) is assumed to be almost perfect. This allows to calculate the weights w_i as

$$w_i = \frac{\left(\sum_{p_\mathrm{T}} N_\gamma^{\mathrm{reco}}(r_i,p_\mathrm{T}) \Big/ \sum_{p_\mathrm{T}} N_\gamma^{\mathrm{reco}}(r_x,p_\mathrm{T})\right)^{\mathrm{DATA}}}{\left(\sum_{p_\mathrm{T}} N_\gamma^{\mathrm{reco}}(r_i) \Big/ \sum_{p_\mathrm{T}} N_\gamma^{\mathrm{reco}}(r_x,p_\mathrm{T})\right)^{\mathrm{MC}}} \tag{5.1}$$

where diffrences in the spectra of initially produced photon numbers in data and mc only have minor effects on the values of the weights.

5.0.1 Choosing the TPC as reference volume

If one wants to put the weights approach into practice a key question is for which radial region of ALICE it is known that the material budget is sufficiently well described in MC. A detector part whose material budget has a comparatively simple structure is the gas within the TPC. If r_x is chosen such that the boarders of the TPC are far enough away given the resolution of the conversion point in R only the gas composition, temperature and pressure need to be properly set in the MC. For this reason, it was decided to choose the fiducial region $90 < R < 150$ cm inside the TPC for the normalization. When investigating this option further it turned out that the TPC gas description in the MC productions was not accurate enough since the gas in the simulations was tuned to standard conditions with the pressure about 4 % lower than the mean pressure present in the cavern. For this reason, the conversion numbers from the TPC in MC need first to be corrected for the deviating atmospheric conditions in MC with respect to the conditions that were present when the data was recorded.

Choosing the TPC as the callibration volume brings with it another intricacy, as the number of reconstructed photon conversions from within the TPC may be biased due to TPC pileup. Pileup denotes the fact, that due to the comparatively long read out time of the TPC of up to 92 μs [8] it may happen that the TPC sees the charged tracks of severall

collisions combined in one read out cycle. In order to minimize the systematic uncertainty on the number of photon conversions due to pileup it was decided to use the runs of the data taking period LHC10b. During this period the luminosity was so low that there was basically no out-of-bunch pileup.

5.0.2 Corrections for the Atmospheric Conditions for LHC10b

According to equation 2.1, in the high momentum limit and for small relative radiation lenghts x/X_0 the photon conversion probability is at first order proportional to the relative radiation length. Since the integrated relative radiation length of the TPC gas is at the order of a percent the linear approximation can be taken. A medium containing nuclei of a certain type has a radiation length X_0 which is proportional to the number density of the nuclei in the medium. According to the equation for an ideal gas:

$$p\,V = N\,k_{\mathrm{B}}\,T \tag{5.2}$$

The number of particles in a given volume is proportional to the quotient $p\,/\,T$. As a consequence, the conversion probability for photons traversing the TPC in the monte carlo simulation will be off by the same factor as $p\,/\,T$ in MC is off compared to the atmospheric conditions while data taking. Figure 5.1 shows the corresponding correction factor $f_{\mathrm{corr}}^{\mathrm{atm}}$:

$$f_{\mathrm{corr}}^{\mathrm{atm}} = \frac{(p\,/\,T)^{\mathrm{DATA}}}{(p\,/\,T)^{\mathrm{MC}}} \tag{5.3}$$

for the runnumbers from the data taking period LHC10b used for the determination of the weights. The correction factors for the single runnumbers were then weighted with the numbers of events to get an overall correction factor applicable to the number of reconstructed photon conversions with the conversion point within the volume used for the callibration. The value of the overall correction factor was found to be $f_{\mathrm{corr}}^{\mathrm{atm}} = 0.963$. For the periods LHC10cdef the averaged value was found to be 0.960 and for this reason the same TPC weight was used for all periods when applying the weights during the analysis.

5.0.3 Calculating the Weights for a variable lower p_{T}-boundary

We have seen in equations 4.16 and 4.19 that the weights can only be as accurate as the V0 reconstruction efficiency in DATA is reproduced by MC and that the photon reconstruction efficiency as determined from MC, when using the weights, will be off by $f_{\mathrm{off}}^{\epsilon_{\mathrm{V0}}}(r_x)$, the factor describing the discrepancy of the V0 reconstruction efficiencies in DATA and MC for the radial bin used as trusted reference volume in MC. In section 4.2 we made the assumption that $f_{\mathrm{off}}^{\epsilon_{\mathrm{V0}}}(r_x)$ does not depend on p_{T} which facilitated the considerations. It seems however likely that there is indeed a p_{T}-dependence of that variable. In addition, the p_{T} shapes of the produced photons might differ, which would also lead to a dependence of the weights on the integration range.

To investigate this, the weights were calculated for diffrent p_{T} integration ranges. Any dependence of the weights on the p_{T} integration range points to a p_{T}-dependence of $f_{\mathrm{off}}^{\epsilon_{\mathrm{V0}}}(r_x)$ or differing shapes of the produced photon spectra. Figure 5.2 shows the weights

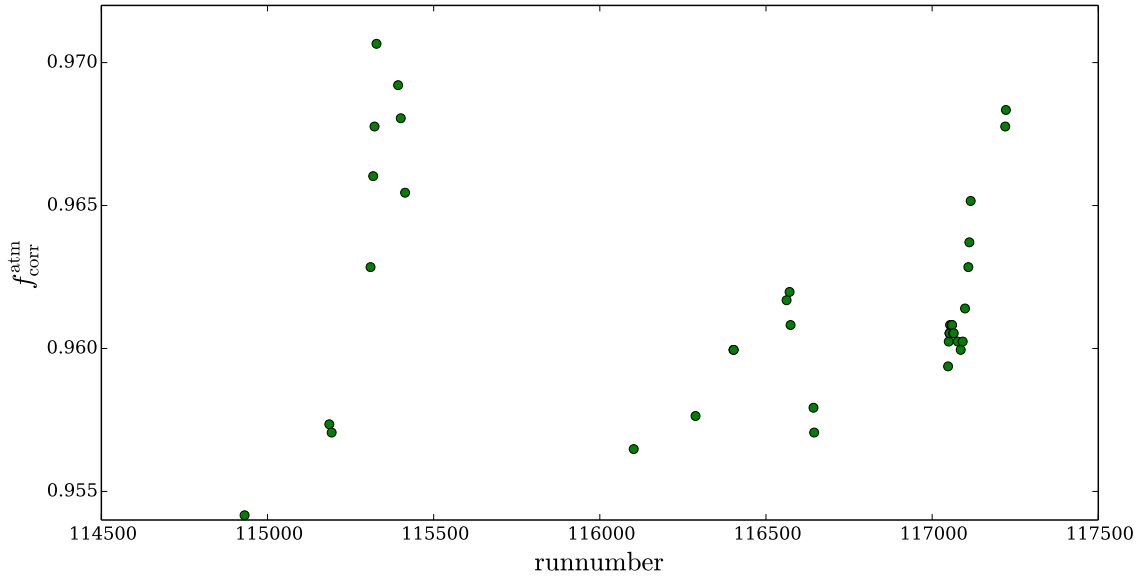

Figure 5.1: Averaged atmospheric correction factors for the runnumbers used for determining the weights.

calculated for various p_{T}-ranges, starting with $p_{\mathrm{T,min}} = 0.0\mathrm{GeV}/c$ and incrementing $p_{\mathrm{T,min}}$ in steps of $0.1\mathrm{GeV}/c$ up to $0.6\mathrm{GeV}/c$, then followed by two $0.2\mathrm{GeV}/c$ steps. The upper integration was kept constant at $16\mathrm{GeV}/c$. It is obvious that the weights do depend on the lower p_{T} limit of the integration range. Figure 5.3 shows the dependence of each of the weights on the lower p_{T} boundary of the integration range.

From inspecting how the weights change with increasing the lower p_{T} boundary it was decided to chose $p_{\mathrm{T,min}} = 0.5\mathrm{GeV}/c$. Figure 5.4 shows the weights calculated for $p_{\mathrm{T,min}} = 0.5\mathrm{GeV}/c$. The weights were calculated for two cutselections with the onfly V0 finder. These are denoted 160 and 161 in the plot. 160 is the standard cut used for the determination of the weight within this thesis and gives a purity between 98 and 99 %. 161 is the same cut as 160 but with an additional cut on $\mathrm{d}E/\mathrm{d}x$ of the electrons in the TPC, yielding a slightly higher purity. 162 is the same cut as 160 but with the offline V0 finder used, yielding a purity even higher.

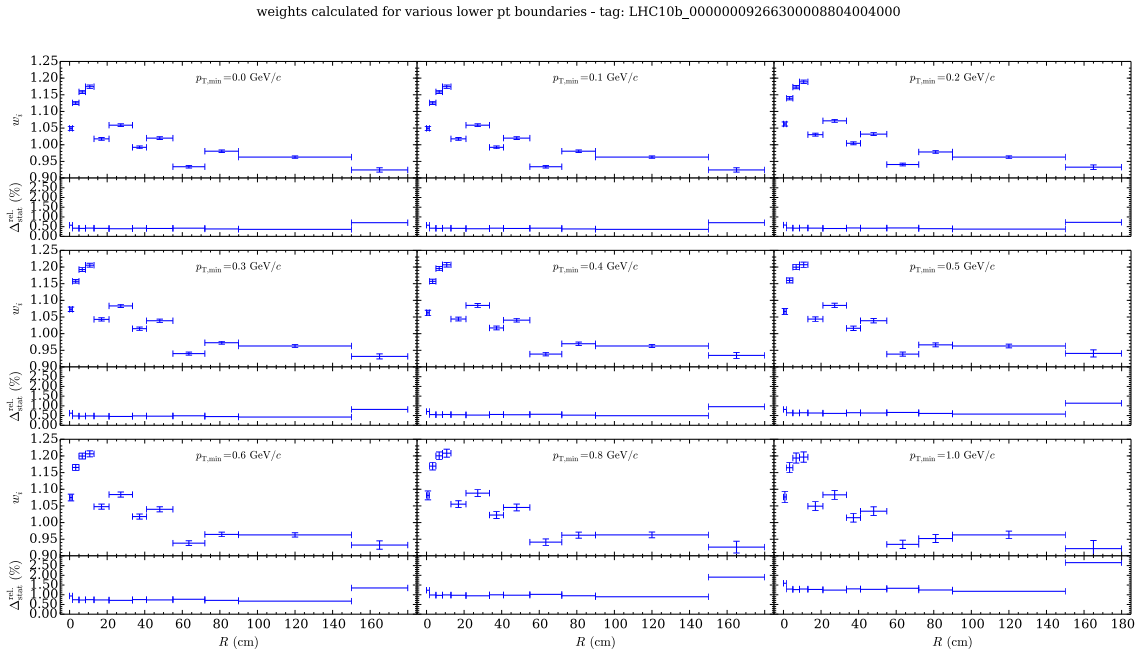

Figure 5.2: Weights calculated for various lower p_T boundaries of the integration ranges. Lower subpanels show the weights' relative statistical uncertainties. Calculated for the data taking period LHC10b. The value of the weight between 90 and 150cm corresponds to the atmospheric correction factor f^{atm}_{corr} that was used. Its statistical uncertainty corresponds to the uncertainty of the ratio of reconstructed photon numbers within the callibration bin between data and MC which and enters the statistical uncertainty of every other bin.

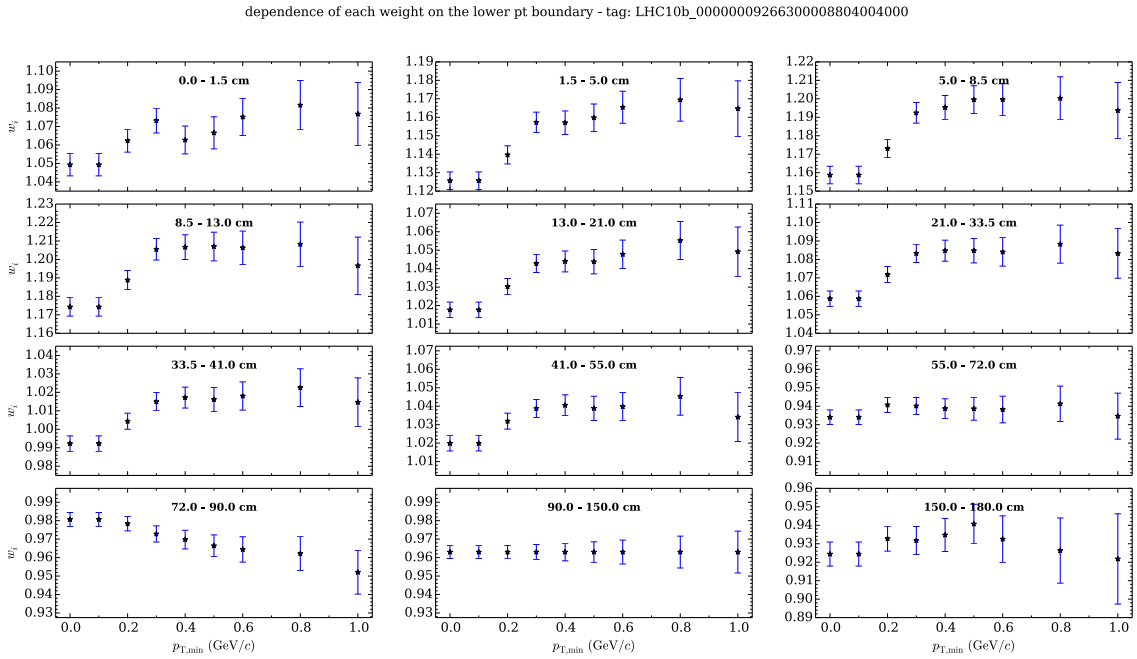

Figure 5.3: Each panel shows the dependence of a certain weight on the lower p_{T} boundary. Calculated for the data taking period LHC10b. The value of the weight between 90 and 150cm corresponds to the atmospheric correction factor $f_{\mathrm{corr}}^{\mathrm{atm}}$ that was used. Its statistical uncertainty corresponds to the uncertainty of the ratio of reconstructed photon numbers within the callibration bin between data and MC which and enters the statistical uncertainty of every other bin.

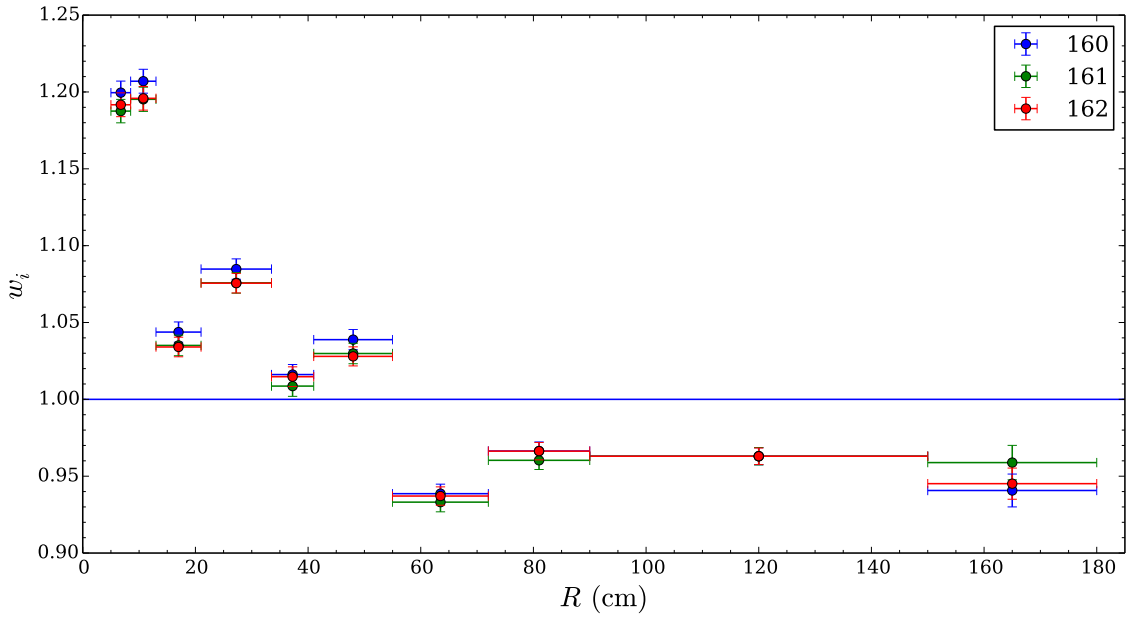

Figure 5.4: Weights calculated for the chosen lower p_{T} boundary of $p_{\mathrm{T,min}} = 0.5\mathrm{GeV}/c$ for the standard cutselection for determining the weights (160), the standard cutselection with an additional $\mathrm{d}E/\mathrm{d}x$ cut on the electrons in the TPC (161) and the standard cutselection with the offline V0-finder used (162).

Chapter 6

Effects of the Weights on the π^0 yield

To study the effect of the weights on actual measurements, the π^0 analyses in the $\gamma\gamma$ and the Dalitz channel were chosen. This allows for comparisons between the two channels and for comparisons to charged pion spectra. The ratio of produced neutral over charged pions can then be compared to the same ratio as predicted by PYTHIA8 tune 4C as an independent check whether the weights are doing something good or not.

6.1 Expected effect on π^0 yield in the two channels

The π^0 meson has two major decay modes which both are exploited in analyses which make use of the PCM: $\pi^0 \to \gamma\gamma$ and $\pi^0 \to e^+e^-\gamma$ with branching ratios of (98.823±0.034)% and (1.174±0.035)% respectively.

6.1.1 Measuring the π^0 yield in the $\gamma\gamma$ channel

In order to demonstrate how the weights can be used in the π^0 analysis and what effects are to be expected, the method for measuring neutral pions in the $\gamma\gamma$ channel is briefly sketched. A more detailed description of the method can be found in [7]. In a first step, a set of photon candidates is determined with the same routine as described in section 3.1. From the set of photon candidates a set of meson candidates is determined by grouping every possible combination of two photon candidates into pairs. The meson candidates are binned in p_{T} according to the summed pair momentum and their invariant mass is calculated from $M_{\gamma\gamma} = \sqrt{2E_{\gamma 1}E_{\gamma 2}(1-\cos\Theta_{12})}$, where Θ_{12} stands for the opening angle between the two photons in the laboratory frame. The pairs with two photons from a common meson mother will have an invariant mass distributed around the mass of the mother meson. The raw yield of reconstructed π^0 mesons is then extracted by integrating the background[1] subtracted signal in a region around the signal peak. The raw yield is then corrected for contributions from pileup and secondaries. In a last step, the fully corrected raw yield of primary π^0 mesons is divided by the detector acceptance and by the π^0 reconstruction efficiency $\epsilon_{\pi^0}^{\mathrm{reco}}(p_{\mathrm{T}})$ to get to total numbers of produced π^0 mesons in a

[1] The expected combinatorial background can be detemined by making use of techniques such as the Event Mixing Method or the Rotation Method

specified rapidity window. The π^0 reconstruction efficiency is determined from MC as:

$$\epsilon_{\pi^0}^{\text{reco}}\left(p_{\text{T}}\right) = \frac{N_{\pi^0}^{\text{reco., verified MC, primary}}\left(p_{\text{T, rec}}\right)}{N_{\pi^0,\,|y_{\pi^0}|<y_{\max},\,|\eta_{\gamma'\text{s}}|<\eta_{\max}}\left(p_{\text{T, MC}}\right)} \tag{6.1}$$

and implicitly corrects for the π^0 momentum resolution. The π^0 reconstruction efficiency is where an inaccurate material budget description in MC will lead to an efficiency deviating from the efficiency when recording data and as a consequence will spoil the final result of the analysis.

6.1.2 How can the weights be applied?

In order to see how weights could be used to correct for an inaccurate material budget description let us have a look on the expectation value of the π^0 meson reconstruction efficiency as determined from MC. The expectation value of reconstructed neutral pions can be written as:

$$\left\langle N_{\pi^0}^{\text{reco}}\left(p_{\text{T}}\right)\right\rangle = \int_0^{p_{\text{T}}} \mathrm{d}p_{\text{T}}^{'} \frac{\mathrm{d}N_{\gamma\gamma\text{ pair}}^{decay}(p_{\text{T}}^{'}, p_{\text{T}} - p_{\text{T}}^{'})}{\mathrm{d}p_{\text{T}}^{'}} \epsilon_{\gamma}^{\text{reco}}(p_{\text{T}}^{'})\, \epsilon_{\gamma}^{\text{reco}}(p_{\text{T}} - p_{\text{T}}^{'}) \tag{6.2}$$

From this equation it seems natural that an inaccurate material budget description in MC can be corrected for by applying the product of photon weights $w_i \cdot w_j$, i, j denoting the radial bins in which the photons converted, when filling the histograms of validated, reconstructed π^0 mesons. Under some simplifying assumptions the effect of the weights can be demonstrated. To this end, we assume the photon reconstruction efficiency in MC can be expressed as

$$\epsilon_{\gamma}^{\text{reco,MC}}\left(p_{\text{T}}\right) = \sum_i f_{\text{off}}^{\epsilon_{\gamma}^{\text{reco}}}\left(r_i\right)\, \epsilon_{\gamma}^{\text{reco}}\left(r_i, p_{\text{T}}\right) \tag{6.3}$$

where we neglect the p_{T}-dependence off $f_{\text{off}}^{\epsilon_{\gamma}^{\text{reco}}}$ any inaccuracy in the MC material budget would induce via $f_{\text{off}}^{p_{\text{r}}}\left(r_i, p_{\text{T}}\right)$ (see section 4.2). We can then write for the number of reconstructed pions in MC when applying the weights:

$$\left\langle N_{\pi^0}^{\text{reco,MC}}\left(p_{\text{T}}\right)\right\rangle^{\text{ww}} = \sum_{i,j} \left\langle N_{\pi^0}^{\text{reco,MC}}\left(p_{\text{T}}\right)\left(r_i, r_j\right)\right\rangle^{\text{ww}} \tag{6.4}$$

$$= \sum_{i,j} \left\langle N_{\pi^0}^{\text{reco,MC}}\left(p_{\text{T}}\right)\left(r_i, r_j\right)\right\rangle \cdot w_i\, w_j \tag{6.5}$$

$$= \sum_{i,j} \int_0^{p_{\text{T}}} \mathrm{d}p_{\text{T}}^{'} \frac{\mathrm{d}N_{\gamma\gamma\text{ pair}}^{decay}(p_{\text{T}}^{'}, p_{\text{T}} - p_{\text{T}}^{'})}{\mathrm{d}p_{\text{T}}^{'}} \cdot f_{\text{off}}^{\epsilon_{\gamma}^{\text{reco}}}\left(r_i\right) \epsilon_{\gamma}^{\text{reco}}(r_i, p_{\text{T}}^{'})\; f_{\text{off}}^{\epsilon_{\gamma}^{\text{reco}}}\left(r_j\right) \epsilon_{\gamma}^{\text{reco}}(r_j, p_{\text{T}} - p_{\text{T}}^{'}) \cdot w_i\, w_j \tag{6.6}$$

From the last equation it is obvious that for a set of weights w_i which are sufficiently close to the inverse of $f_{\text{off}}^{\epsilon_{\gamma}^{\text{reco}}}\left(r_i\right)$ the expectation value of reconstructed pions in MC

$\left\langle N_{\pi^0}^{\mathrm{reco,MC}}(p_{\mathrm{T}})\right\rangle^{\mathrm{ww}}$ will be close to what one would obtain if one had the same photon reconstruction efficiency in MC as in DATA.

6.1.3 Predicted effect of weights on π^0 yield

As will be shown in section 6.2, the observed effect of the weights on the π^0 yield exhibits a non-negligible p_{T}-dependence. In the following it will be shown that a p_{T}-dependence with similar shape and order of magnitude can be explained by the fact that the p_{T}-shape of the photon reconstruction efficiency changes with the conversion radius of the photons. The bottom panel of figure 6.1 shows the predictable strongly p_{T}-dependent impact of the weights on both the photon reconstruction efficiency and the π^0 reconstuction efficiency. The ratio of the photon reconstruction efficiencies steeply increases for $p_{\mathrm{T}} < 0.3\,\mathrm{GeV/c}$ up to values even larger than unity. This can be understood if one studies both the R-distributions of reconstructed photons for diffrent p_{T} bins, as depicted in figure 6.2, and the values of the weights, as were shown in figure 5.4. Between 0.1 and 0.4 Gev/c the share of the low R radial bins to the total reconstruction efficiency increases considerably. While for the p_{T}-bin $0.1 < p_{\mathrm{T}} < 0.2\,\mathrm{GeV/c}$ the total reconstruction efficiency is almost completely determined by $i_x - 1$, where $i_x - 1$ is an identifier for the bin next to the callibration bin towards low R, the share of $i_x - 1$ to the total photon reconstruction efficiency decreases going to higher p_{T}. As a consequence, the effect of the weights on the efficiency for p_{T}<0.2 GeV/c is determined by $w_{x-1} \approx 0.96$ while going to larger p_{T} also the low R weights with values up to 1.2 enter the total recontruction efficiency with substantial weight.

To get to the expected effect of the weights on the π^0 reconstruction efficiency, recall that it is determined from the ratio of reconstructed over produced π^0 mesons. The distribution of produced $\gamma\gamma$ decay pairs $\mathrm{d}N^{decay}_{\gamma\gamma\,\mathrm{pair}}(p_{\mathrm{T}}^{'}, p_{\mathrm{T}} - p_{\mathrm{T}}^{'})/\mathrm{d}p_{\mathrm{T}}^{'}$ in equation 6.6 is proportional to the p_{T}-distribution of produced π^0 mesons. We can hence express the expectation value for the observed π^0 reconstuction efficiency in MC when using weights as

$$\left\langle \epsilon_{\pi^0}^{\mathrm{reco,mc}}(p_{\mathrm{T}})\right\rangle^{\mathrm{ww}} = BR \int_0^{p_{\mathrm{T}}} \mathrm{d}p_{\mathrm{T}}^{'}\, g(p_{\mathrm{T}}^{'}, p_{\mathrm{T}} - p_{\mathrm{T}}^{'})\, \epsilon_{\gamma}^{\mathrm{reco,MC,ww}}(p_{\mathrm{T}}^{'})\, \epsilon_{\gamma}^{\mathrm{reco,MC,ww}}(p_{\mathrm{T}} - p_{\mathrm{T}}^{'}) \tag{6.7}$$

where BR denotes the branching ratio, $g(p_{\mathrm{T}}^{'}, p_{\mathrm{T}} - p_{\mathrm{T}}^{'})$ the probability density function that the daughter photons of a decaying π^0 with transverse momentum p_{T} have $p_{\mathrm{T}}^{'}$ and $p_{\mathrm{T}} - p_{\mathrm{T}}^{'}$ transverse momentum and $\epsilon_{\gamma}^{\mathrm{reco,MC,ww}}$ the observable MC photon reconstuction efficiency when using weights. The middle panel of figure 6.1 shows the predicted π^0 reconstruction efficiencies with and without the weights based on a numerical integration of equation 6.7. To this end, the photon reconstruction efficiencies were fitted with functions of the form

$$f(p_{\mathrm{T}}) = \frac{b \cdot \left(1.0 - e^{-\frac{p_{\mathrm{T}} - e}{a}}\right)}{1.0 + e^{\frac{p_{\mathrm{T}} - c}{d}}} \tag{6.8}$$

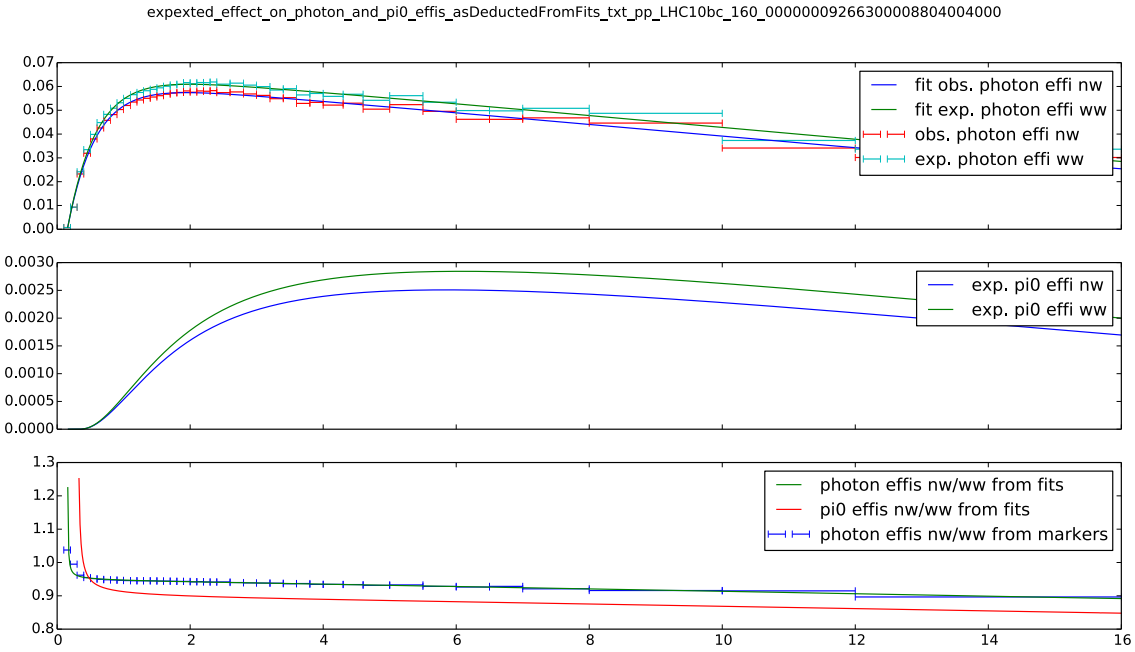

Figure 6.1: Top panel: nw markers show the observed photon reconstruction efficiency in the data sample used for determining the weights. ww markers show the photon reconstruction efficiency as it would be observed from the same data sample when using the weights. The lines are fits of the form as in equation 6.8. Middle panel: Calculated expected π^0 reconstruction efficiencies using the fitted photon reconstruction efficiencies from the top panel as input for a numerical integration of equation 6.7. Bottom panel: lines: ratios of photon and π^0 reconstruction efficiencies with and without weights from top and middle panels. They show the expected effect of the weights on the photon and π^0 reconstruction efficiencies. markers: Ratio of photon reconstruction efficiencies (markers) in top panel. They serve as sanity check for the quality of the fits for the photon reconstruction efficiencies. Ideally, these markers should lay on the line showing the ratio of fitted photon reconstuction efficiencies.

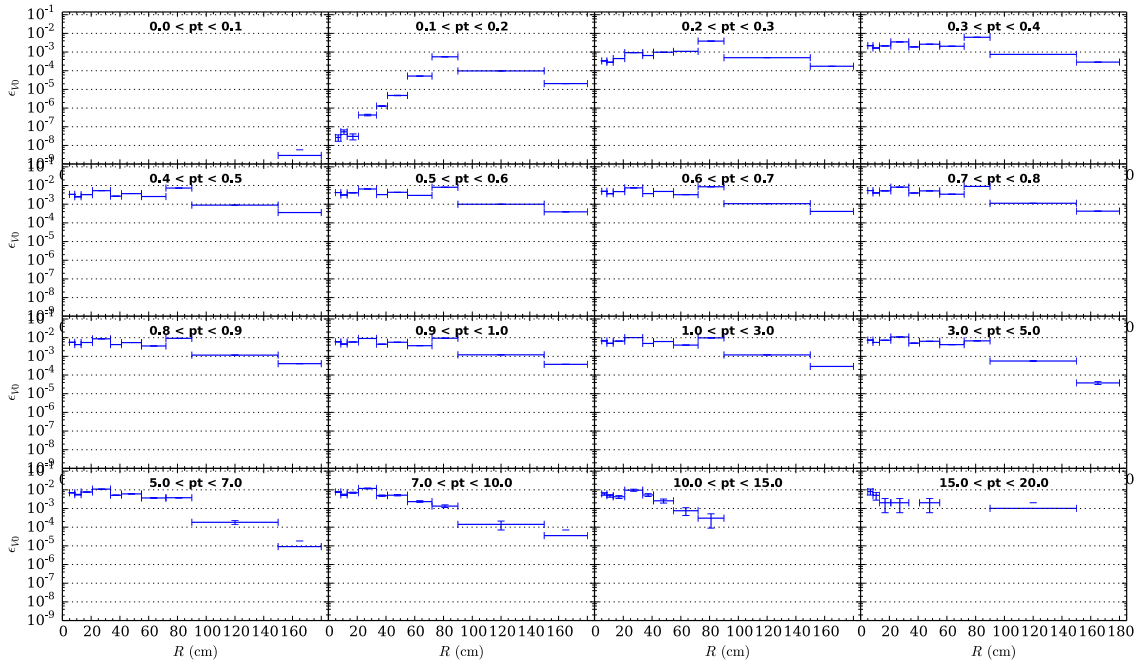

Figure 6.2: R distributions of photon reconstruction efficiecies in p_{T} bins. Same data sample as used for the determination of the weights.

and $g(p_{\mathrm{T}}^{'}, p_{\mathrm{T}} - p_{\mathrm{T}}^{'})$ was approximated by $g(p_{\mathrm{T}}^{'}, p_{\mathrm{T}} - p_{\mathrm{T}}^{'}) = \frac{1}{p_{\mathrm{T}}}$ [2], the probability density for observing a photon with transverse momentum p_{T} after a π^0 decay which had transverse momentum $p_{\mathrm{T},\,\pi^0}$. The fits are plotted in the top panel of figure 6.1

6.2 Observed Effect on π^0 yields

6.2.1 Observed effect in $\gamma\gamma$ channel

Figures 6.3 and 6.4 show the observed effect of the weights on the π^0 yield in the $\gamma\gamma$ channel for pp and pPb. For pp, the observed effect is compared to predictions for this effect, that are based only on the photon reconstruction efficiency that was observed when determining the weights. The prediction reproduces the strong p_{T}-dependence of the observed effect. The ratio of invariant π^0 meson yields from $\gamma\gamma$ over $ee\gamma$ in pPb is not shown since the statistical uncertainties are so high that one can not make any statment if the ratio is closer to unity with our without the weights.

[2] This approximation is valid since the line on which the photons fly away from the decaying π^0 is distributed isotropically in the π^0's rest frame.

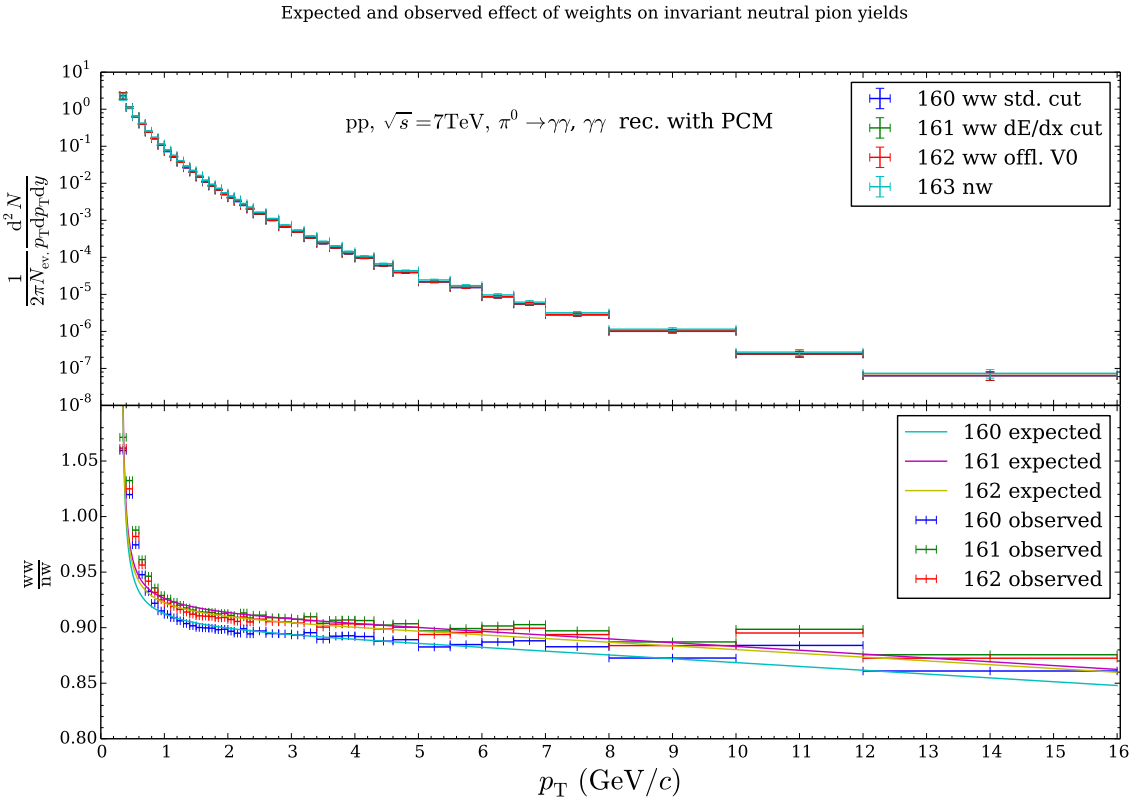

Figure 6.3: Top panel: Markers 160 - 162: Observed π^0 invariant yields for three sets of weights determined with varying photon cuts: 160 - standard cut, 161 - standard cut with TPC electron dE/dx cut, 162 - standard cut with offline V0-finder. Markers 163: Observed π^0 invariant yields without weights. Bottom panel: Markers: Ratios of observed π^0 invariant yields with weights over no weights for the three sets of weights. Lines: Prediction for ratios of observable π^0 invariant yields with weights over no weights for the three sets of weights based on the photon reconstruction efficiency observed for the standard cut that was used for determinig the weights.

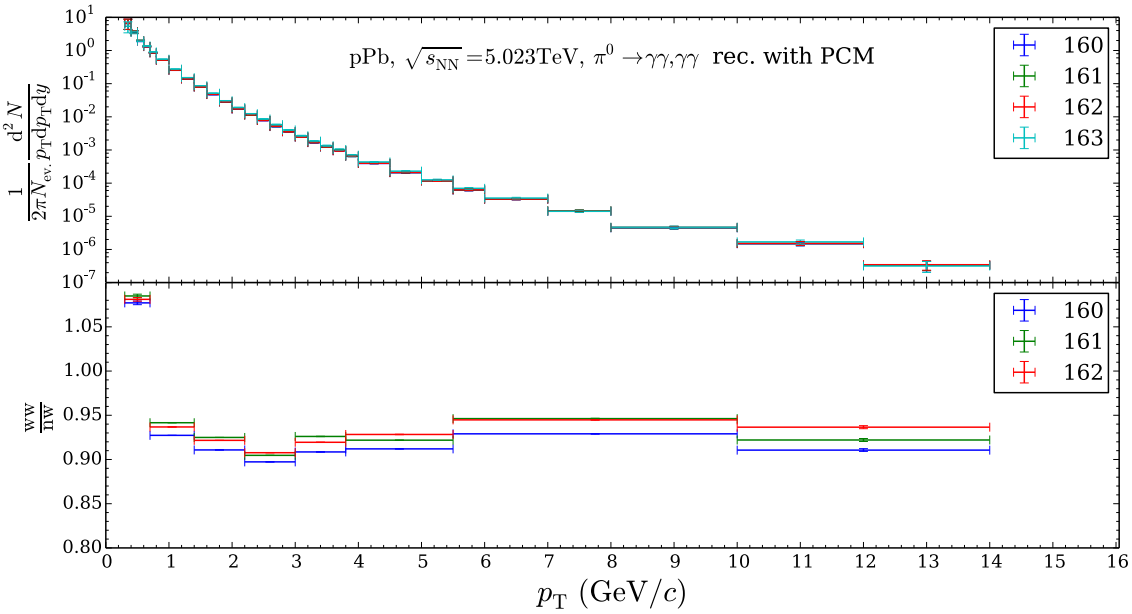

Figure 6.4: Top panel: Markers 160 - 162: Observed π^0 invariant yields for three sets of weights determined with varying photon cuts: 160 - standard cut, 161 - standard cut with TPC electron dE/dx cut, 162 - standard cut with offline V0-finder. Markers 163: Observed π^0 invariant yields without weights. Bottom panel: Ratios of observed π^0 invariant yields with weights over no weights for the three sets of weights.

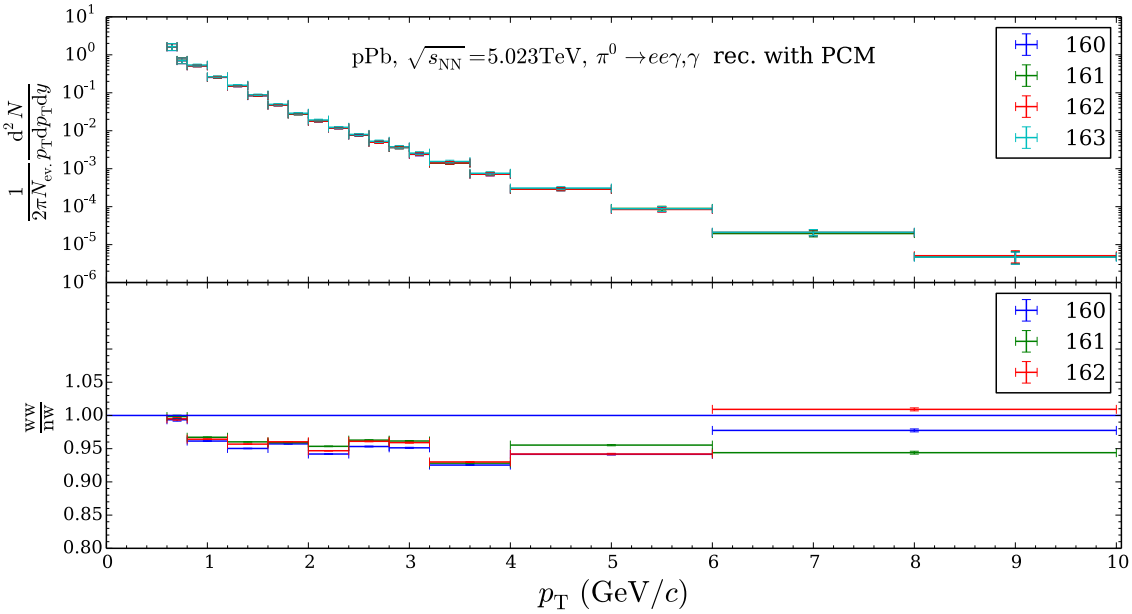

Figure 6.5: Top panel: Markers 160 - 162: Observed π^0 invariant yields for three sets of weights determined with varying photon cuts: 160 - standard cut, 161 - standard cut with TPC electron dE/dx cut, 162 - standard cut with offline V0-finder. Markers 163: Observed π^0 invariant yields without weights. Bottom panel: Ratios of observed π^0 invariant yields with weights over no weights for the three sets of weights.

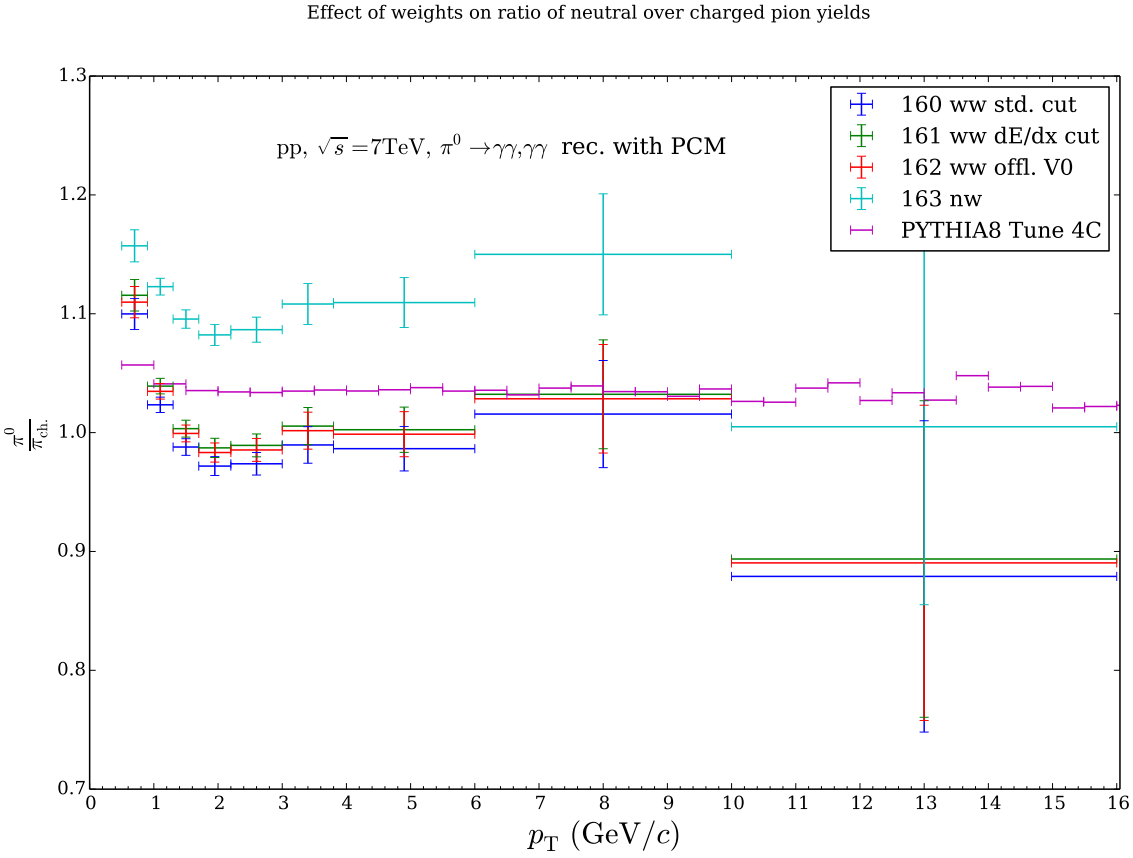

Figure 6.6: Ratios of observed neutral over charged pion yields for three sets of weights determined with varying photon cuts: 160 - standard cut, 161 - standard cut with TPC electron dE/dx cut, 162 - standard cut with offline V0-finder. Markers 163: Observed π^0 invariant yields without weights. Markers 164: Ratio as predicted by PYTHIA8 tune 4C. There is a 5 % systematic uncertainty on markers 160 - 163 arising from the measured charged pion spectrum which is not shown here.

Chapter 7

Summary and Outlook

The weights approach has the potential to reduce the systematic uncertainty of the Photon Conversion Method. It was shown that when using the weights, the material budget will be governed by $f_{\text{off}}^{p_c}(r_x) \cdot f_{\text{off}}^{\epsilon_{\text{V0}}}(r_x)$. Hence, The basic assumption that has to be taken for the approach to be justified, is that there is a region in the detector that (a), has a well understood material budget and (b), in which the V0-efficiency in MC is as well reproduced as in the other regions. While (a) can be assessed from considering the physical structure of ALICE it is difficult to make solid statements about (b). What can be said is that there is no obvious reason why the V0 efficiency should be significantly worse reproduced in the TPC than elsewhere. Moreover, it was shown that when using the weights a systematic error source arises if diffrences in the p_{T} shapes of the produced photon spectra exist. For the investigated scenarios the uncertainty due to this was comparable to the error obtained when no weights were used. In the actual determination of the weights with the TPC gas acting as the callibration volume, the lower limit of the integration range was chosen such that the individual weights were stable for a variation of the limit. If the shapes of the input spectra were considerably diffrent, a stability of the weights while varying the limit would be unlikely.

In order to put the weights approach into practice, the option for using the weights in the analyses of neutral mesons was implemented into the analysis tasks. The effects of the weights on the π^0 yield were studied for pp and pPb collisions. As a check for the implementaion of the weights, the observed effect in pp collisions was compared to a prediction based on a R, p_{T} parametrization of the single photon reconstruction efficiency and found to be in agreement. As a next step, it should be interesting to compare the findings of the callibration with the TPC to the normalization to charged particles that was used up to know for assesing the material budget uncertainty. Moreover, other ways of calculating weights using the TPC come to mind, such as calculating the weights differential in R and p_{T} first and to calculate from these an average over p_{T} in a second step. This would have the advantage of being far less sensitive to differing p_{T} shapes of the produced photon spectra in data and mc.

Bibliography

[1] S. L. Glashow. "Partial Symmetries of Weak Interactions". In: *Nucl. Phys.* 22 (1961), pp. 579–588. DOI: 10.1016/0029-5582(61)90469-2.

[2] S. Weinberg. "A Model of Leptons". In: *Phys. Rev. Lett.* 19 (21 Nov. 1967), pp. 1264–1266. DOI: 10.1103/PhysRevLett.19.1264. URL: http://link.aps.org/doi/10.1103/PhysRevLett.19.1264.

[3] A. Salam. "Weak and Electromagnetic Interactions". In: *Conf. Proc.* C680519 (1968), pp. 367–377.

[4] MissMJ. *Standard Model of Elementary Particles*. 2016. URL: https://commons.wikimedia.org/wiki/File:Standard_Model_of_Elementary_Particles.svg (visited on 12/01/2016).

[5] A. Collaboration et al. "ALICE: Physics Performance Report, Volume II". In: *Journal of Physics G: Nuclear and Particle Physics* 32.10 (2006), p. 1295. URL: http://stacks.iop.org/0954-3899/32/i=10/a=001.

[6] K. Koch. "Measurement of pi0 and eta mesons with photon conversions in ALICE in proton-proton collisions at sqrt(s)=0.9, 2.76 and 7 TeV". PhD thesis. Heidelberg University, 2011.

[7] F. Bock. "Neutral Pion and Eta Meson Production in pp and Pb–Pb Collisions at the LHC with the ALICE Detector". MA thesis. Heidelberg University, 2012.

[8] J. Alme et al. "The ALICE TPC, a large 3-dimensional tracking device with fast readout for ultra-high multiplicity events". In: *Nucl. Instrum. Meth.* A622 (2010), pp. 316–367. DOI: 10.1016/j.nima.2010.04.042. arXiv: 1001.1950 [physics.ins-det].

Erklärung:

Ich versichere, dass ich diese Arbeit selbstständig verfasst habe und keine anderen als die angegebenen Quellen und Hilfsmittel benutzt habe.

Heidelberg, den 20.01.2017 .....